

Strain-engineered A-type antiferromagnetic order in YTiO_3 : a first-principles calculation

Xin Huang,¹ Yankun Tang,¹ and Shuai Dong^{1,2}

¹*Department of Physics, Southeast University, Nanjing 211189, China*

²*Laboratory of Solid State Microstructures, Nanjing University, Nanjing 210093, China*

(Dated: 16 November 2012)

The epitaxial strain effects on the magnetic ground state of YTiO_3 films grown on LaAlO_3 substrates have been studied using the first-principles density-functional theory. With the in-plane compressive strain induced by LaAlO_3 (001) substrate, A-type antiferromagnetic order emerges against the original ferromagnetic order. This phase transition from ferromagnet to A-type antiferromagnet in YTiO_3 film is robust since the energy gain is about 7.64 meV per formula unit despite the Hubbard interaction and modest lattice changes, even though the A-type antiferromagnetic order does not exist in any RTiO_3 bulks.

PACS numbers: 75.25.Dk, 75.30.Kz

Transition metal oxides with the perovskite structure exhibit a wide variety of electronic phases with plenty charge-, magnetic-, and orbital-structures, and show many prominent functionalities including colossal magnetoresistance, high- T_C superconductivity, and metal-insulator transitions.^{1,2} Among these oxides, the RTiO_3 family (R is a rare earth cation), whose $3d\ t_{2g}$ bands lay near the Fermi level, have not been extensively studied. However, RTiO_3 is not a feature-less family, which also owns rich spin/orbital ordered phases.³ These phases also involve the couplings between charge, orbital, lattice, and spin degrees of freedom, which have the potential to be used in spintronic or correlated-electron devices.

RTiO_3 's with trivalent R cations are all prototype Mott-Hubbard insulators and their common crystal structure is a pseudocubic perovskite with an orthorhombic distortion (the GdFeO_3 -type distortion). This distortion arises from the tilting TiO_6 octahedron around the $[110]$ axis and a followed rotation around the $[001]$ axis. The magnitude of this distortion depends on the ionic radii of R . Similar to the RMnO_3 case, the lattice structure is more distorted with a small R and the Ti-O-Ti bond angle is decreased more significantly from 180° . The GdFeO_3 -type distortion plays a crucial role in controlling the subtle competitive exchange interactions in these insulating titanates. The magnetic ground state of RTiO_3 exhibits a transition from ferromagnetic (FM) order to antiferromagnetic (AFM) one with increasing size of R cation.^{4,5}

It is very interesting to compare the phase diagrams of RTiO_3 and RMnO_3 , both of which show magnetic transitions with increasing size of R cations. And the Curie (or Néel) temperatures show V-shape behaviors near the critical points in both families. However, there are also two key differences between RTiO_3 and RMnO_3 . First, the FM-AFM tendency is opposite in these two families. With a smaller R , RMnO_3 is more AFM but RTiO_3 is more FM. Second, the phases revealed in RMnO_3 are more complex than those in RTiO_3 . The AFM phase in RTiO_3 bulks is the simple G-type AFM one while the AFM phases (e.g. A-type AFM, spiral-spin order, E-type

AFM) in RMnO_3 are more complex which can be more interesting than the simple G-type one.⁶ Thus it is non-trivial to ask whether is there any more (hidden) magnetic orders in RTiO_3 ? In a previous theoretical work Ref. 7, total energies of different magnetic structures including A-type AFM, FM and G-type AFM were calculated by using an effective spin-pseudospin Hamiltonian, which showed that the A-type AFM to FM phase transition occurs with increasing GdFeO_3 -type distortion while the G-type AFM one has much higher energies. However, this result disagrees with the experimental phase diagram since the G-type AFM phase is very robust in RTiO_3 with large R while the A-type AFM phase has not been observed in any real RTiO_3 compounds so far.

In this paper, by using the first-principles calculations, we intend to investigate the effects of strain on magnetic structures of YTiO_3 film, focusing on the phase transition of the magnetic ground state. Our calculation predicts that a robust A-type AFM phase can be stabilized by an in-plane compressive strain by using small lattice substrates like LaAlO_3 .

YTiO_3 bulk has a orthorhombic structure (space group $Pbnm$) with lattice constants of $a=5.358\text{ \AA}$, $b=5.696\text{ \AA}$, and $c=7.637\text{ \AA}$. Such a minimum unit cell consists of 4 formula units. To simulate the effect of in-plane compressive strain induced by the substrate, the lattice constants along the a-axis and b-axis are fixed to $a=b=5.366\text{ (}3.794 \times \sqrt{2}\text{) \AA}$ to match the (001) LaAlO_3 substrate. Here LaAlO_3 is adopted as the substrate to give a weak in-plane compressive strain to YTiO_3 film since the in-plane lattice constant of LaAlO_3 is a little smaller ($\sim 3\%$) than that of YTiO_3 itself. Such a small difference between lattice constants also promises probable epitaxial growth of YTiO_3 thin films on LaAlO_3 substrate.

Our first-principles calculations were performed using density-functional theory (DFT) within the generalized gradient approximation GGA+U method^{8,9} with the Perdew-Becke-Erzenhof parametrization¹⁰ as implemented in the Vienna *ab initio* simulation package (VASP).^{11,12} The valence states include $4d^1 5s^2$, $3d^2 4p^2$

TABLE I. The energy difference ΔE (per Ti) between magnetic states and the NM state for unstrained bulk YTiO_3 : $E(\text{magnetic}) - E(\text{NM})$, in unit of eV and the corresponding local magnetic moments per Ti in unit of μ_B .

Magnetic order	NM	FM	A-AFM	C-AFM	G-AFM
ΔE	0	-0.533	-0.530	-0.527	-0.526
Magnetic moment	0	0.88	0.86	0.83	0.82

and $2s^2 2p^4$ for Y, Ti and O, respectively. The lattice optimization and all other static computations have been done with the Hubbard U on the d -electrons of Ti^{3+} ion, and the Dudarev¹³ implementation with $U_{\text{eff}} = 3.2$ eV has been used if not noted explicitly.¹⁴ The atomic positions are fully optimized as the Hellman-Feynman forces are converged to less than $1.0 \text{ meV}/\text{\AA}$. This optimization and the electronic self-consistent iterations are performed using the plane-wave cutoff of 500 eV and a $9 \times 9 \times 6$ Monkhorst-Pack k -point mesh¹⁵ centered at Γ grid in combination with the tetrahedron method.¹⁶

First, the ground state of YTiO_3 bulk is checked. Using the experimental crystal structure, non-magnetic (NM) state and four magnetic orders: FM, A-type AFM, C-type AFM and G-type AFM, have been calculated to compare the energies. Within GGA+ U , our calculations confirm that the FM order has the lowest energy and the calculated local magnetic moment is $0.88\mu_B/\text{per Ti}$ in agreement with the experimental magnetic moment ($0.84\mu_B$).¹⁷ The detail results of calculated total energy are summarized in Table I. According to Table I, other magnetic orders' energies (per Ti) are higher than the FM one: 3 meV higher for A-type AFM, 6 meV higher for C-type AFM and 7 meV higher for G-type AFM. It should be noted that the FM ground state is robust within a large region of U_{eff} from 0 eV to 5 eV (not shown here). Thus, our calculations agree quite well with the experimental results and previous DFT studies.^{14,18}

Subsequently, DFT calculations with the epitaxial strain are performed. Epitaxial strain is here realized by fixing the in-plane lattice constants to fit the LaAlO_3 substrate as stated before, while the lattice constant along c -axis is varied from 7.0 \AA to 9.0 \AA to search the equilibrium one under the strain, as shown in Fig. 1(a). In our calculations, the internal atomic positions are relaxed with magnetism under each fixed lattice framework to obtain optimal crystal structures for calculating accurate energies. According to Fig. 1(a), it is obvious that the C-type AFM and G-type AFM states are much higher in energy than the FM and A-type AFM states. Thus, in the following, we will mainly focus on the FM and A-type AFM states. The relaxed lattice constant along c -axis is 8.25 \AA for the A-type AFM state and 8.26 \AA for the FM state. These two values are very close, implying that the magnetostriction is weak in YTiO_3 , at least along the c -axis. And with the optimized c -axis lattice constant, the A-type AFM state has a lower energy than FM one, e.g. the energy difference between FM and A-

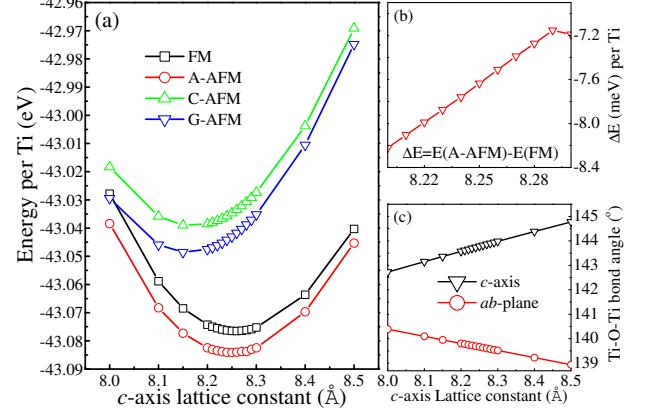


FIG. 1. (Color online) (a) Energies for different magnetic orders as a function of the c -axis lattice constant. (b) The energy difference between the A-type AFM and FM as a function of the c -axis lattice constant. (c) The Ti-O-Ti bond angle in ab -plane and along the c -axis respectively for the A-type AFM state.

type AFM reaches 7.64 meV per Ti. The A-type AFM state appeared in strained YTiO_3 films is quite nontrivial since it does not exist in any RTiO_3 bulk, namely it is a new phase for RTiO_3 family. More importantly, this strain-induced phase transition from FM to A-type AFM is quite promising according to our calculation. As shown in Fig. 1(b), the energy difference between these two orders does not change sign for a large range of c -axis lattice constant around the optimized one, which means this transition is not sensitive to the optimized c -axis lattice constant. Noted that the energy difference is relatively significant since the energy difference in bulk YTiO_3 is only 3 meV per Ti. To confirm that this phase transition is robust against the change of Hubbard parameter, the energy difference between FM and A-type AFM states is calculated with different U_{eff} from 0 eV to 5 eV stepped by 1 eV, which changes from 16 meV to 2 meV (always positive). In other words, this FM to A-type AFM transition will not change by varying the Hubbard interaction U_{eff} in a large value (from 0 eV to 5 eV). In short, this strain-induced A-type AFM phase will be very promising to be found in real thin films even if the experimental lattice constant along c -axis and its Hubbard interaction are not exactly the same with those in our calculations.

To understand the underlying physical mechanism, it is meaningful to compare the Ti-O-Ti bond angle in YTiO_3 with and without the strain, as shown in Table. II. According to Fig. 1(c), the bond angle in the ab -plane decreases but the one along c -axis increases with the increasing c -axis. These results imply that YTiO_3 is compressed and thus more distorted in the ab -plane but elongates and thus is less distorted along the c -axis.

As stated before, it is well known that in RTiO_3 compounds, small Ti-O-Ti bond angles with more dis-

TABLE II. Bond angles in the ab -plane and along c -axis of YTiO_3 film on LaAlO_3 substrate and bulk YTiO_3 .

Ti-O-Ti bond angle	YTiO_3 film (A-AFM)	YTiO_3 film (FM)	bulk YTiO_3 (FM)
ab -plane	139.6°	139.5°	144.3°
c -axis	143.7°	143.5°	141.9°

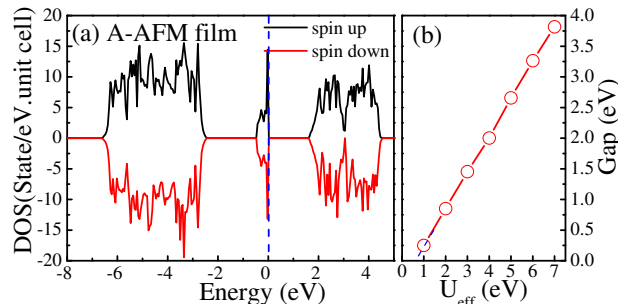


FIG. 2. (Color online) (a) Total DOS of YTiO_3 film. The Fermi energy is positioned at zero. (b) The energy gap as a function of U_{eff} . The critical U_{eff} value for zero gap is estimated as 0.6 eV by extrapolation.

torted lattice structure exhibit FM order while those with larger Ti-O-Ti bond angle tend to be AFM. It should be noted that this tendency is in opposite to the tendency in manganites. In manganites, the straighter (closer to 180°) bond angle should lead to ferromagnetic exchange. Therefore, the strain driven phase transition here is not exactly the same with the corresponding one in strained manganites.¹⁹ So here in strained case, the spin order in ab -plane has a tendency towards FM correlation due to decreasing in-plane Ti-O-Ti bond angle, while the increasing bond angle along c -axis tends to drive spins arranged antiparallel. In this sense, the emergence of A-type AFM in YTiO_3 on LaAlO_3 substrate can be qualitatively understood as the ferromagnetism with decreasing bond angle in ab -plane and antiferromagnetism with increasing bond angle along c -axis. Of course, a comprehensive understanding of this magnetic transition needs more careful studies from microscopic theory. Furthermore, the bond angles are very close between FM and A-AFM states in strained films, implying that the exchange-striction effect is weak in this materials, which is different from the strong exchange-striction in manganites²⁰ or ion-selenides.²¹

In many correlated electron materials, accompanying magnetic transitions, conductance often changes drastically, e.g. metal-insulator or insulator-superconductor transitions. Therefore, it is necessary to check the density of states (DOS) of YTiO_3 under strain, as shown in Fig. 2(a).

First of all, YTiO_3 bulk is an insulator in our DFT calculation (not shown here), in agreement with the ex-

perimental result.³ This insulating behavior is due to the Coulomb repulsion between $3d$ electrons, implying a Mott insulator. This scenario can be easily demonstrated because the pure GGA calculation without the Hubbard U gives a metallic DOS. The band gap is 1.504 eV for bulk YTiO_3 , a little overestimated compared with the experimental data 1.2 eV.²² Our calculation found a gap as 1.564 eV for YTiO_3 under strain, which is only a little larger than the bulk value. This gap exists within a wide range of U_{eff} from 1 eV to 7 eV, though the detail value depends on U_{eff} , as shown in Fig. 2(b). Therefore, it is safe to say that the strained YTiO_3 remains an insulator and its conductance is not obviously changed since the gaps are almost identical.

In summary, we have studied the effects of epitaxial strain on the magnetic ground states in YTiO_3 films. Our results predicted a new magnetic ground phase A-type antiferromagnet which had not been realized in any RTiO_3 bulk compounds. This robust A-type AFM phase is stabilized by an in-plane compressive strain induced by LaAlO_3 substrate. Its origin is understood as the ferromagnetism with decreasing bond angle in the ab -plane and antiferromagnetism with increasing bond angle along the c -axis. Furthermore, the density of states calculation confirmed that the insulating behavior and the energy gap would not be significantly affected by this strain driven magnetic transition.

We thank X. Z. Lu, H. J. Xiang, Q. F. Zhang, H. M. Liu for helpful discussion. Work was supported by the 973 Projects of China (Grant No. 2011CB922101) and NSFC (Grant Nos. 11004027 and 11274060).

- ¹E. Dagotto, Science **309**, 257 (2005).
- ²Y. Tokura, Rep. Prog. Phys. **69**, 797 (2006).
- ³M. Mochizuki and M. Imada, New J. Phys. **6**, 154 (2004).
- ⁴T. Katsufuji, Y. Taguchi, and Y. Tokura, Phys. Rev. B **56**, 101454 (1997).
- ⁵J. E. Greedan, J. Less Common Met. **111**, 335 (1985).
- ⁶S. Dong, R. Yu, S. Yunoki, J.-M. Liu, and E. Dagotto, Phys. Rev. B **78**, 064414 (2008).
- ⁷M. Mochizuki and M. Imada, J. Phys. Soc. Jpn. **70**, 1777 (2001).
- ⁸P. E. Blöchl, Phys. Rev. B **50**, 17953 (1994).
- ⁹G. Kresse and D. Joubert, Phys. Rev. B **59**, 1758 (1999).
- ¹⁰P. Perdew, K. Burke, and M. Ernzerhof, Phys. Rev. Lett. **77**, 3865 (1996).
- ¹¹G. Kresse and J. Hafner, Phys. Rev. B **47**, 558 (1993).
- ¹²G. Kresse and J. Furthmüller, Phys. Rev. B **54**, 11169 (1996).
- ¹³S. L. Dudarev, G. A. Botton, S. Y. Savrasov, C. J. Humphreys, and A. P. Sutton, Phys. Rev. B **57**, 1505 (1998).
- ¹⁴H. Sawada, Y. Morikawa, K. Terakura, and N. Hamada, Phys. Rev. B **56**, 12154 (1997).
- ¹⁵H. Monkhurst and J. D. Pack, Phys. Rev. B **13**, 5188 (1976).
- ¹⁶P. E. Blöchl, O. Jepsen, and O. K. Andersen, Phys. Rev. B **49**, 16223 (1994).
- ¹⁷J. D. Garrett, J. E. Greedan, and D. A. MacLean, Mater. Res. Bull. **16**, 145 (1981).
- ¹⁸H. Sawada, N. Hamada, and K. Terakura, Physica B **237**, 46 (1997).
- ¹⁹J. H. Lee and K. M. Rabe, Phys. Rev. Lett. **104**, 207204 (2010).
- ²⁰S. Picozzi, K. Yamauchi, B. Sanyal, I. A. Sergienko, and E. Dagotto, Phys. Rev. Lett. **99**, 227201 (2007).
- ²¹W. Li, S. Dong, C. Fang, and J. P. Hu, Phys. Rev. B **85**, 100407 (2012).

²²Y. Okimoto, T. Katsufuji, T. Arima, and Y. Tokura, Phys. Rev. B **51**, 9581 (1995).